Reservoir pressure analysis of aortic blood pressure: an in-vivo study at five locations in humans

Narayan, Om[a,e]; Parker, Kim H.[b]; Davies, Justin E.[c]; Hughes, Alun D.[d]; Meredith, Ian T.[a,e]; Cameron, James D.[a,e]

[a]Monash Cardiovascular Research Centre, Monash University, Melbourne, Australia

[b]Department of Bioengineering

[c]International Centre for Circulatory Health, Imperial College

[d]UCL Institute of Cardiovascular Science, University College, London, UK

[e]MonashHeart, Monash Health, Victoria, Australia

Correspondence to James D. Cameron, MD, MBBS, BE, MEngSc, FCSANZ, Monash Cardiovascular Research Centre, Monash Medical Centre, 246 Clayton Road, Clayton, VIC 3168, Australia.

E-mail:james.cameron@monash.edu

Abbreviations: BP, blood pressure (mmHg); cBP, central blood pressure; DBP, diastolic blood pressure; ICC, intra-class correlation coefficient; kd, diastolic rate constant (/s); ks, systolic rate constant (/s); LV, left ventricle; P(t), measured pressure waveform (mmHg); P[infinity], asymptotic pressure for diastolic pressure fall-off (mmHg); Pd, diastolic (minimum) pressure (DBP) (mmHg); Pn, pressure at the end of systole (mmHg); Pr(t), reservoir pressure waveform (mmHg); Pr max, maximum of Pr(t) above Pd (mmHg); Ps, systolic (peak) pressure of pressure wave (SBP) (mmHg); Px(t), excess pressure waveform (mmHg); Px max, maximum of Px(t) (mmHg); Qin, volume flow rate into the aortic root (m3/s); SBP, systolic blood pressure; SD, standard deviation; SE, standard error; T, cardiac period (s); Td, diastolic period (s); Tn, systolic period (s); Tr, time of Pr max (s); Ts, time of Ps (s); Tx, time of Px max (s)

Abstract

Introduction: The development and propagation of the aortic blood pressure wave remains poorly understood, despite its clear relevance to major organ blood flow and potential association with cardiovascular outcomes. The reservoir pressure model provides a unified description of the dual conduit and reservoir functions of the aorta. Reservoir waveform analysis resolves the aortic pressure waveform into an excess (wave related) and reservoir (compliance related) pressure. The applicability of this model to the pressure waveform as it propagates along the aorta has not been investigated in humans.

Methods: We analysed invasively acquired high-fidelity aortic pressure waveforms from 40 patients undergoing clinically indicated coronary catheterization. Aortic waveforms were measured using a solid-state pressure catheter at five anatomical sites: the ascending aorta, the transverse aortic arch, the diaphragm, the level of the renal arteries, and at the aortic bifurcation. Ensemble average pressure waveforms were obtained for these sites for each patient and analysed to obtain the reservoir pressure [Pr(t)] and the excess pressure [Px(t)] at each aortic position.

Results: Systolic blood pressure increased at a rate of 2.1 mmHg per site along the aorta, whereas diastolic blood pressure was effectively constant. Maximum Pr decreased only slightly along the aorta (changing by -0.7 mmHg per site), whereas the maximum of Px increased from the proximal to distal aorta (+4.1 mmHg per site; $P < 0.001$). The time, relative to the start of systolic upstroke, of the occurrence of the maximum excess pressure did not vary along the aorta. Of the parameters used to derive the reservoir pressure waveform the systolic and diastolic rate constants showed divergent changes with the systolic rate constant (ks) decreasing and the diastolic rate constant (kd) increasing along the aorta.

Conclusions: This analysis confirms the proposition that the magnitude of the calculated reservoir pressure waveform, despite known changes in aortic structure, is effectively constant throughout the aorta. A progressive increase of excess pressure accounts for the increase in pulse pressure from the proximal to distal aorta. The reservoir pressure rate constants seem to behave as arterial functional parameters. The accompanying decrease in ks and increase in kd are consistent with a progressive decrease in aortic compliance and increase in impedance. The reservoir pressure waveform therefore provides a model that might have utility in understanding the generation of central blood pressure and in specific cases might have clinical utility.

INTRODUCTION

The physiology of aortic pressure propagation and its dysfunction in disease states is of considerable potential clinical significance. Indeed central blood pressure (cBP) has been suggested to better predict cardiovascular and cerebral events than traditionally measured brachial BP [1–4]. Derangements in cBP may also be associated with excessive pressure propagation to more distal arteries with associated abnormalities including renal dysfunction amongst other common abnormalities [5–7]. Aortic root BP is a determinant of the response of coronary blood flow to adenosine, both before and after angioplasty, and therefore is a likely determinant of impaired cardiac function and coronary flow reserve in addition to its well known association with left ventricular hypertrophy [8]. An enhanced understanding of the mechanisms underlying central aortic pressure generation and the propagation of the pressure wave distally is a necessary prerequisite for the improved management of chronic medical conditions including stroke, chronic coronary syndromes and renal disease.

Traditional paradigms of aortic pressure generation are based on the assumption that aortic pressure is the sum of a single forward-travelling and a single backward-travelling reflected pressure waveform [9]. More recent theories have modified this concept and stressed the relevance of increased proximal aortic stiffness and aortic diameter, accompanied by decreased impedance mismatch as being more relevant in determining the magnitude of aortic BP than reflected wave phenomena [5].

An alternative approach to describing central aortic function is provided by the reservoir-wave hypothesis. This heuristic hypothesis states that it may be useful to treat the aortic pressure waveform, P(t), as the summation of a reservoir pressure waveform, Pr(t), which accounts for the net compliance of the arteries, and an excess pressure waveform, Px(t), which is determined by local waves [10]. Implicit in this hypothesis is the assumption that Pr(t) is made up from myriad minuscule forward and backward wave fronts. These derive from the forward travelling waves generated in the aortic root by the left ventricle, but are modified by reflection and re-reflection as they travel through the arterial circulation [11]. The reservoir-wave hypothesis was developed to explain experimental observations in the canine circulation [12] where it has been shown to resolve a number of anomalies that arise in traditional impedance-based analysis. One anomaly is the observation that the forward and backward pressure waveforms are large and equal in magnitude during late diastole [12,13]; this assumption is necessary to explain the exponentially decreasing fall in pressure at a time when the flow rate is negligible. These large ‘standing’ waves, if present, should, however, be evident in transient conditions such as in the presence of ectopic or missing beats when ‘standing’ waves have not had time to die away; in fact, it is regularly observed that the exponential fall in pressure continues

smoothly from late diastole into the prolonged period before the next, delayed, systole. An advantage of the reservoir pressure concept is that virtually all of the measured pressure during diastole is attributed to Pr so that the excess pressure during diastole is very close to zero, matching the diastolic flow [10,13,14]. This obviates the need for the invocation of a large, self-cancelling backward pressure waveform during diastole to account for the fall in pressure while the flow is zero.

We and others have suggested that central pressure waveform morphology may be due to cardiac or left ventricular outflow tract which influences to a greater extent than to effects related to distal wave reflection. Our earlier results relating to the systolic inflection point, traditionally taken as the temporal indication of the arrival back into the central aorta of a reflected pressure wave during systole, were not consistent with the wave reflection model, occurring later at more distal sites rather than earlier as would be expected if it was due to a backward-travelling wave [15]. Similarly, in a meta-analysis performed by Baksi et al.[16], the timing of the systolic pressure wave inflection point was not found to shift markedly from diastole to systole with ageing. Other modelling studies have also challenged the contention that pressure wave reflection is the predominant mechanism driving pressure wave augmentation, instead suggesting left ventricular outflow and local vessel mechanical properties may play an important role [17,18].

Potential conceptual advantages of the reservoir pressure model include that reservoir pressure is affected by global cardiovascular properties, for example, total compliance and net resistance, whereas excess pressure varies with location and could be a sensitive indicator of local conditions or focal pathology. Utilization of these differences may provide useful clinical insight [19].

It is possible to derive the reservoir pressure using only the local measured pressure without need of the clinically more difficult measurement of local flow [20]. This pressure-only reservoir pressure algorithm depends on the assumptions that the reservoir pressure waveform is uniform as it propagates throughout the arteries and that the flow waveform at the aortic root is proportional to the excess pressure waveform [21]. Excess pressure Px(t), defined as the difference between P(t) and Pr(t), may be potentially a better indicator of local wave behaviour, because the complexities due to the global storage and release of blood associated with compliant arteries is accounted for by the reservoir pressure. Neither of these assumptions has been tested in the human aorta.

We therefore hypothesized that application of reservoir pressure analysis to the recorded waveforms from well defined anatomical levels may provide further insight into the underlying mechanism of pressure wave propagation in the aorta.

METHODS

Forty participants (26 men) were studied at the time of coronary angiography (32 participants) or percutaneous coronary intervention (8 participants) at MonashHeart in Melbourne, Australia. The study was approved by the Institutional Human Research and Ethics Committee, and performed in accordance with institutional guidelines. Participants gave written informed consent. All participants were in sinus rhythm at the time of the study.

Data acquisition

Data were acquired following completion of the clinically indicated procedure. Aortic waveforms were acquired using a 2 French Millar Mikro-tip catheter transducer introduced via a 6 French multipurpose or right coronary guiding catheter positioned at the aortic root under fluoroscopic control. The Millar transducer was positioned just distal to the tip of the guiding catheter. Waveforms were recorded at a sampling rate of 2000 Hz to Chart for PowerLab (ADInstruments, Australia), decimated to 200 Hz for analysis. Following the acquisition of 30 s of data from the aortic root, the guiding catheter and Millar transducer were pulled back together, and similar data were recorded at the level of the transverse aortic arch, the diaphragm, the renal arteries, and at the aortic bifurcation sequentially. All positions were confirmed by fluoroscopy, and the levels of the renal arteries and aortic bifurcation were determined by angiography. The physical distance between recording sites was measured by the use of a marker catheter; however, all results are reported in terms of anatomical landmarks (rather than absolute distances) as these provide reproducible and specific structural discontinuities unrelated to patient height. The electrocardiogram was recorded simultaneously with all pressure measurements. Mean arterial pressure (MAP) was calculated as the integral mean over the ensemble average pressure cycle.

Ensemble averaging and calculation of the reservoir pressure

An automatically generated ensemble average of individual cardiac cycles was used in analysis. The cycle averaged standard deviation (SD) of the ensemble averages was 4.4 mmHg, which did not vary by site. Because not all pressure waveforms, particularly those from the more distal sites, exhibited a dicrotic notch, the time of end of systole, Tn, was determined as the time of the minimum dP/dt after the systolic (peak) pressure. The average duration of the cardiac period (T) is derived from the fundamental peak of the power spectrum of the time series from which the ensemble averages were calculated.

The reservoir pressure, Pr(t), was calculated from the ensemble average measured pressure, P(t). The algorithm assumes that Pr satisfies overall conservation of mass:

$$\frac{dP_{\mathrm{r}}}{dt} + k_{\mathrm{d}}(P_{\mathrm{r}} - P_{\infty}) = \frac{Q_{in}}{C} \qquad (1)$$

where kd is the diastolic rate constant (the reciprocal of the diastolic time constant [tau] = RC, where R is the net resistance to flow through the microcirculation and C is the net compliance of the arteries). Qin is the volume flow rate into the aortic root and P[infinity] is the asymptote of the diastolic pressure fall-off. If we further assume that Px = [zeta] Qin, then Eq. (1) can be written as follows:

$$\frac{dP_{\mathrm{r}}}{dt} + k_{\mathrm{d}}(P_{\mathrm{r}} - P_{\infty}) = k_{\mathrm{S}}(P - P_{\mathrm{r}}) \qquad (2)$$

where ks is the systolic rate constant (the reciprocal of [zeta]C). This first-order linear differential equation can be solved as follows:

$$P_{\mathrm{r}} = \mathrm{e}^{-(k_{\mathrm{S}}+k_{\mathrm{d}})t} \int_0^t P(t')\mathrm{e}^{(k_{\mathrm{S}}+k_{\mathrm{d}})t'}\,\mathrm{d}t' + \frac{k_{\mathrm{d}}}{k_{\mathrm{S}}+k_{\mathrm{d}}} \times \left(1 - \mathrm{e}^{-(k_{\mathrm{S}}+k_{\mathrm{d}})t}\right) P_{\infty} \qquad (3)$$

The diastolic parameters kd and P[infinity] are obtained first by fitting an exponential curve to P during diastole and ks is obtained by minimizing the square error between P and Pr obtained over diastole.

Statistical analysis

All continuous variables are presented as their mean ± SD, unless otherwise indicated. Significance was taken as P less than 0.05. The agreement between parameters describing the P, Pr, and Px waveforms was summarized using the intra-class correlation coefficient (ICC) function (Stata 13.1; StataCorp, College Station, Texas, USA) derived from a linear mixed-model analysis with participant as a random effect and location included as an ordinal fixed effect rather than a continuous variable. This is appropriate to our data because the aortic sites were defined relative to anatomical locations, not measured distances.

Because the beta coefficient (slope) is dimensional (with the same dimensions per unit ordinal scale increase in location as the intercept), it is useful to define the % slope as percentage of the intercept to give a measure of the relative size of the variation in the parameter from site to site. Further statistical analysis was performed using SPSS 11.0 for Windows (SPSS Inc., Chicago, Illinois, USA) and Stata (StataCorp).

RESULTS

Participant characteristics are described in Table 1. Participants were predominantly men (n = 26, 65%), mean age was 65 ± 12 years, mean height 170 ± 8 cm, mean weight 79 ± 14 kg, and mean BMI 28 ± 5 kg/m2. Ten percent were current smokers, 22% had hypertension, 22.5% had diabetes mellitus, 55% were hypercholesterolemic, and 22.5% had a family history of cardiovascular disease. Twenty-two percent had no significant coronary disease on angiography; and 35%, 16%, and 27% had single-vessel, double-vessel, and triple-vessel disease, respectively. Left ventricular function was assessed in 22 of 40 participants and was normal in 20 of 22 (91%). These characteristics are representative of individuals presenting for coronary investigation in our service.

Number	40
Male sex, *n* (%)	26 (65%)
Age (years)	65 ± 12
Height (m)	1.70 ± 0.08
Weight (kg)	79 ± 14
BMI (kg/m^2)	28 ± 5
Percutaneous coronary intervention, *n* (%)	8 (20%)
Smoking (current), *n* (%)	4 (10%)
Hypertension, *n* (%)	22 (55%)
Diabetes mellitus, *n* (%)	9 (23%)
Hypercholesterolaemia, *n* (%)	34 (85%)
Family history CVD, *n* (%)	9 (23%)

CVD, cardiovascular disease.
Continuous variables are mean ± SD.

TABLE 1 Participant characteristics

Complete pulse wave analysis of these results has been reported previously [15]. All except one of the participants exhibited a pre-systolic BP (SBP) inflection point with average augmentation pressure 23 ± 17 mmHg in the aortic root taken, in conventional wave-reflection models, to be associated with increased aortic stiffness and early return of any reflected wave. This is consistent with the age and clinical presentation of the cohort studied.

Parameters describing the measured pressure

Parameters describing the pressure waveforms are defined in Fig. 1, which shows the ensemble average pressure waveform (solid line) at the aortic bifurcation site in one of the patients. It also shows the calculated reservoir pressure, Pr (dashed line), and excess pressure Px (dotted line). To make comparisons easier, the measured and reservoir pressures are plotted relative to the diastolic

pressure. Fig. 2(a) shows the ensemble average of the measured pressure (solid line) at the five aortic sites for one patient, together with the reservoir (dashed) and excess (dotted) pressures. Time zero corresponds to the time of the peak of the R-wave of the simultaneously measured ECG. The thin solid line represents the time at the diastolic point (the start of systole) at each site. The slope of this line is the pulse wave velocity, which, as can be seen, is fast compared to the rate of changes of the pressure waveforms. Figure 2(b) shows data from the same individual participant showing pressure waveforms at the five sites relative to atmospheric pressure (left panel), which illustrates that there were changes in Pd between sites. The right hand panel shows the same data plotted relative to Pd [i.e. P(t) - Pd and Pr(t) - Pd).

The measured pulse pressure increases distally. The Pr waveform fits the diastolic pressure very closely, and so Px, defined as the difference between P and Pr, is effectively zero throughout diastole.

The blood pressure and pulse wave analysis parameters at the five aortic sites have been previously reported [15]. In brief, augmentation index and augmentation pressure decreased with propagation distally from the aortic root, whereas the pressure at the systolic inflection point progressively increased. SBP and diastolic BP (DBP) increased and remained constant, respectively, moving away from the ascending aorta towards the aortic bifurcation.

Table 2 shows the parameters derived from the waveform analysis at the five measurement sites. The parameters include the systolic pressure Ps, the diastolic pressure Pd, and the pressure at the end of systole Pn.

		P_s (mmHg)	P_d (mmHg)	$P_{r,max}$ (mmHg)	T_r (ms)	$P_{x,max}$ (mmHg)	T_x (ms)	T_w (ms)	P_∞ (mmHg)	Pn (mmHg)	k_s (/s)	k_d (/s)
Aortic position	Ascending	131.8	65.2	49.4	59	25.3	28	64.0	54.5	115.8	15.39	2.68
	Arch	129.7	64.6	47.5	57	26.5	25	62.7	54.4	113.8	14.00	2.52
	Diaphragm	140.5	69.6	49.07	56	31.8	25	60.6	59.4	122.9	12.20	2.73
	Renal	139.2	67.1	47.24	54	36.1	24	59.4	58.3	119.4	10.46	2.87
	Bifurcation	141.6	66.8	47.16	54	39.4	25	59.1	58.8	120.4	9.78	3.06

k_d, diastolic rate constant; k_s, systolic rate constant; P_d, diastolic pressure; P_n, pressure at the end of systole; P_∞, asymptotic fall-off pressure; $P_{r,max}$, maximum reservoir pressure; P_s, systolic pressure; $P_{x,max}$, maximum excess pressure; T_n, time to end of systole; T_r, time to $P_{r,max}$; T_x, time to $P_{x,max}$.

TABLE 2 Summary of mean reservoir pressure parameters by aortic location

The parameters derived from linear mixed-model analysis of the ensemble average pressure waveforms at the five aortic sites are given in Table 3, and showed excellent agreement (ICC > 0.9) between locations. The cardiac period, T, was unchanged, consistent with haemodynamic stability over the period of measurements. Despite the close agreement between aortic sites, there was a

significant variation of the reservoir pressure parameters by location (Tables 3–5). A main finding of this analysis relates to the systolic and diastolic rate constants describing aortic behaviour (Table 4). The diastolic rate constant, kd, increased from the aortic root to the bifurcation. Conversely, ks, the systolic rate constant, decreased at all levels in the aorta, from the aortic root to the bifurcation. The fractional slope of kd from site to site was 6.7%, which corresponds to slightly more than a 25% increase from the root to the aortic bifurcation. Similarly, the asymptote of the diastolic pressure fall-off increased by nearly 10%, and ks decreased by more than a third between the aortic root and the aortic bifurcation (Fig. 3). Inspection of the 95% confidence estimates for the slope suggests this is unlikely to be accounted for by chance.

	P_s (mmHg)	P_d (mmHg)	P_n (mmHg)	T_n (ms)	T (ms)
Intercept	133.6 (126.7, 140.5)	68.2 (65.2, 71.2)	119.3 (113.9, 124.7)	333.0 (321, 345)	976.0 (926, 1025)
Slope	2.13 (1.66, 2.59)	0.06 (−0.24, 0.36)	0.71 (0.24, 1.17)	−6.0 (−7.0, 5.0)	−2.0 (−8.0, 3.0)
% slope	1.6%	0.1%	0.6%	−1.8%	−0.2%
ICC	0.96	0.91	0.93	0.98	0.96

ICC, intra-class correlation coefficient; P_d, diastolic BP; P_n, pressure at the end of systole; P_s, systolic BP; T, cardiac cycle length; T_n, time of the end of systole relative to the previous end diastole.
Intercept – the intercept of the linear mixed model for the five aortic sites for all patients; slope – the beta coefficient of the linear mixed model, % slope – 100 × slope/intercept.

TABLE 3 Linear mixed model analysis of the reservoir pressure parameters measured at the five aortic sites

	k_d (/s)	P_∞ (mmHg)	k_s (/s)
Intercept	2.26 (1.86, 2.66)	54.3 (50.7, 57.9)	17.3 (15.6, 18.9)
Slope	0.152 (0.067, 0.237)	1.22 (0.78, 1.66)	−1.61 (−1.96, −1.26)
Fractional slope	6.7%	2.2%	−9.3%
ICC	0.99	0.90	0.94

ICC, intra-class correlation coefficient; k_d, diastolic rate constant; k_s, systolic rate constant; P_∞, asymptote of the exponential diastolic pressure fall-off.
The intercept and slope are given as mean (95% confidence interval).
Intercept – the intercept of the linear mixed model for the five aortic sites for all patients; slope – the beta coefficient of the linear mixed model, % slope – 100 × slope/intercept.

TABLE 4 Linear mixed-model analysis of the parameters used in the calculation of P_r

	$P_{r\,max} - P_d$ (mmHg)	T_r (ms)	$P_{x\,max}$ (mmHg)	T_x (ms)	IP_x (mmHg s)	IP_r (mmHg s)
Intercept	52.1 (47.8, 56.3)	308 (297, 318)	20.1 (16.6, 23.5)	144 (125, 163)	4.9 (3.91, 5.90)	21.7 (19.8, 23.6)
Slope	−0.68 (−1.01, 0.34)	−6 (−7, −5)	4.09 (3.64, 4.54)	−3 (−7, 1)	0.7 (0.61, 0.80)	−0.38 (−0.55, 0.23)
Fractional slope	−1.3%	1.9%	20.4%	−2.1%	14.3%	−1.8%
ICC	0.98	0.96	0.96	0.91	0.97	0.97

ICC, intra-class correlation coefficient; IP_r, the integral of $(P_r - P_d)$ over the cardiac period; IP_x, integral of P_x over the cardiac period; $P_{r\,max}$, maximum of P_r; $P_{x\,max}$, maximum of P_x; T_r, time to $P_{r\,max}$ over the cardiac period; T_x, time to $P_{x\,max}$.
The intercept and slope are given as mean (95% confidence interval).
Intercept – the intercept of the linear mixed model for the five aortic sites for all patients; slope – the beta coefficient of the linear mixed model, % slope, 100 × slope/intercept.

TABLE 5 Linear mixed-model analysis of the parameters describing P_r and P_x

Reservoir and excess pressure parameters

The change in the reservoir pressure from site to site in the aorta can be described by a number of parameters. In Table 2, we report the peak value of the reservoir pressure relative to the diastolic pressure Pr rmax, and the time of the peak value Tr. The percentage slopes of the parameters related to Pr are relatively small (Table 5), Pr max - Pd reduces by -1.3% and Tr increases by 1.9% between measurement sites. Relative to the change in Pr, there was a large variation of Px over the five aortic sites, with 20.4% change in the maximum excess pressure (Px max) per site distally. This is accompanied by a change in the time to the peak (Tx) by -2.1% per site. These results for the site to site variation of the peaks of P, Pr and Px are shown graphically in Fig. 3.

Supplementary Fig. 1 shows the mean (±SD) of the correlation coefficients of the four pair-wise correlations of the reservoir pressure waveform at the distal sites against the aortic root waveform. The grand average of all patients is 0.989 ± 0.001 [standard error of mean (SEM)], strongly supporting consistence of reservoir pressure within individuals.

Although P(t) = Pr(t) + Px(t), the peaks in the different waveforms occur at different times and so Ps is not equal to the sum of Pr max and Px max. Comparing the results for both reservoir and excess pressure, we note that Px max occurs significantly earlier than Pr max, and that this difference increases at the more distal sites.

DISCUSSION

The reservoir-wave hypothesis is relatively new and remains controversial with some arguing that the concepts are inappropriate or incorrect [22].

On the basis of a number of erroneous assumptions, Westerhof et al.[22] concluded that Pr = 2Pb, where Pb is the backward wave [9,23]. Whereas this relationship is true during diastole, it is not true during systole when the two pressure separation methods give different results. Other concerns have been raised by Mynard and Smolich [24], based on anomalies in the computed results of Pr in various highly simplified models of the arterial system, for example, a single bifurcation or a single tapering tube. These models lack the homogenizing effect of highly dispersed reflection sites (bifurcations and terminal impedances) that are present in physiological arteries. These computational studies do raise interesting questions (and provide the means for exploring them), but we do not believe that inconsistencies of the reservoir-wave hypothesis in simplified, idealistic models indicate that it is not applicable in real arteries.

Other reservations about the reservoir-wave concept are contained in the study by Segers et al.[25], in which the applicability of reservoir pressure analysis in younger individuals is queried. We believe that these criticisms must be taken seriously and are suggestive of the studies that are essential to determine the utility of the reservoir-wave hypothesis, which is ultimately the only way of testing this heuristic hypothesis. To address these issues further, we have included an expanded technical discussion as part of the 'Supplementary Material' accompanying this study.

On the contrary, there are now a number of retrospective clinical studies that have looked at the prognostic value of various parameters derived from Pr and Px[19,26,27]. In all of these studies looking at different patient populations, a reservoir pressure parameter (e.g. integral of Px, peak Pr, etc.) has been shown to have significant prognostic value, which generally persists after other risk factors have been factored into the analysis. These studies do not, of course, indicate that the reservoir pressure concept is 'right', but do provide a strong argument for the utility of the reservoir-wave hypothesis. The question of clinical relevance and potential application of the reservoir pressure concept is an important one.

We feel that the clinical novelty and potential utility of the reservoir pressure analysis lies in the fact that reservoir pressure analysis provides quantitative metrics that are more sensitive to the systolic phase of the pressure generation. The time constant of diastolic pressure decay is effectively independent of systolic function. Parameters based on augmentation pressure and forward and backwards wave decomposition, although manifest in a systolic waveform, are taken as associated with distal arterial properties associated with reflection and not indicative of true systolic behaviour. Because the reservoir pressure accounts for virtually all of the diastolic pressure, it follows that the excess pressure should be more sensitive to the ventriculo-vascular interaction during systole. Clinically measureable metrics based on the reservoir and excess pressure may therefore be uniquely sensitive to derangement of the interaction between volume inflow and the mechanical response of the arteries. In a growing number of studies, reservoir pressure analysis has provided quantifiable metrics that have been shown to have independent prognostic value.

The reservoir pressure parameters describing systolic features, for example, systolic rate constant (ks) and excess pressure (Pex), do hold potential for further investigation in other populations and may provide an easily measurable metric that indicates systolic performance. If so, this would be a considerable benefit in both mechanistic and interventional studies and potentially in patient care. Of

note, in regard to patient care was the suggestion in the study by Narayan et al. that the reservoir parameter systolic rate constant ks seemed to predict likelihood of response to diuretic versus angiotensin-converting enzyme inhibitor (ACEI)-based therapy in elderly hypertensive patients.

This is the first description of reservoir analysis applied at precise anatomical sites in the human aorta using pressure waveforms acquired with invasive, high-fidelity, solid-state transducers. The application of this model to the in-vivo human data of this study provides insights into haemodynamic influences contributing to aortic blood pressure at different sites. It also provides a check of the self-consistency of the basic assumption that Pr is uniform throughout the arterial system.

Reservoir pressure

The parameters used to calculate the reservoir and hence the excess pressures, ks, kd, and P[infinity], vary from site to site in the aorta; however, the Pr waveform (Table 5 and Fig. 3) exhibits only a small and insignificant variation as it propagates along the aorta. For example, Pr rmax decreased by 0.68 mmHg per site, with a 95% confidence interval (CI) which included zero. The agreement between sites was also very close (ICC > 0.97). The near uniformity of the reservoir pressure waveform calculated at different sites along the human aorta is consistent with similar measurements made in the canine aorta [10].

The site-by-site variation in ks, kd and P[infinity], although small, were larger than expected at the outset of the study. Each of these parameters has a physical meaning. The value kd is the reciprocal of the exponential time constant and P[infinity] is the asymptote that the pressure would reach if diastole was extended indefinitely. Both of these parameters are obtained by fitting the ensemble average pressure decay during diastole. The value ks is the reciprocal of the product of the constant of proportionality ([zeta]) between the excess pressure and the volume flow rate at the aortic root, and the global compliance (C) of the arterial system.

Given the physical meaning of these parameters, changes in the cardiovascular system due to ageing or disease might result in their derangement. This study was not designed to explore this possibility directly but provides indications that this might be a productive avenue for future research.

We conclude that the maximum and shape of the Pr(t) waveform calculated from the measured pressure is effectively constant as it transverses the aorta (fractional slope of Pr max = -1.3% per site). This is in contrast to the peak excess pressure which increased by 4.1 mmHg per site (fractional slope 20.4% per site). The constancy of Pr and the large variation of Px along the aorta supports the basic assumption that Pr depends on global properties of the arterial system, whereas Px depends on local properties. Being able to separate local from global effects will inevitably increase our understanding of the mechanism responsible for the aortic pressure waveform and could be advantageous in clinical measurements of the effects of pathological or pharmacological changes.

In addition to decreasing in compliance, the aorta tapers with distance from the aortic root – the effect of branching vessels is to channel off proximal aortic blood volume, for example, via brachial, subclavian, inter-costal, renal, mesenteric, and so on arteries – with the more distal aortic pulse pressure determined by the incrementally advancing volume of blood, a decreasing cross-sectional area and increasing local stiffness. Anything less than an ideal match of these local properties, for example, associated with ageing, will result in a mismatched haemodynamic result likely associated with an increased local BP. Reservoir pressure analysis suggests that mismatch between blood volume and aortic compliance causes an increase in local excess pressure and hence local pulse pressure. This is consistent with ageing and disease-related processes that have been well identified, but importantly, it also suggests that such changes can be better understood in terms of local effects without any discernible influence from distal arterial segments [11] or of a predominant single reflected wave as postulated in models based on a uniform tube assumption [28].

Limitations

The patients in the study are representative of patients undergoing clinical diagnosis in a catheter laboratory, but are not necessarily representative of the population as a whole. We have no data on reservoir pressure in the aorta in younger patients, and therefore cannot definitively comment on whether our results are generalizable to all cohorts; we, however, feel that it is likely that the results can potentially be extrapolated to the general population with reasonable confidence.

Reservoir waveform analysis involves a number of assumptions relating to the aortic pressure waveform, including that waveform decay measured at different aortic locations is similar in diastole. Secondly, it assumes that the excess pressure waveform is proportional to the flow waveform at the

aortic root. Given these two assumptions, reservoir pressure can be calculated solely from the pressure waveform, without requirement for assessment of flow. Our results need to be interpreted within these inherent assumptions, and further work is needed to address these assumptions. Our current study has, however, demonstrated a substantial degree of self-consistency.

In conclusion, elevations in central and aortic pulse pressure are associated with incident cardiovascular events. Wave reflection is widely considered to contribute significantly to aortic pulse pressure through pulse pressure augmentation. Based on reservoir-pressure analysis, local wave transmission seems to play a relatively larger role in the distal aortic pressure waveform (as indicated by increasing excess pressure), whereas the reservoir pressure waveform (determined by global aortic compliance) plays a greater role at the ascending aorta.

The major insights from this analysis are that the calculated reservoir pressure waveform (peak and shape), despite known changes in aortic structure and biomechanical properties, is effectively uniform throughout the aorta; the increase in pulse pressure in more distal locations of the aorta is attributable to increasing excess pressure; and that the systolic and diastolic rate constants increase and decrease respectively along the aorta. This variation in the rate constants suggests that they are related to intrinsic functional properties and, as such, may have prognostic implications. The reservoir pressure waveform can provide a description that might have utility in understanding generation of BP and might have clinical utility in specific cases.

ACKNOWLEDGEMENTS

Conflicts of interest

There are no conflicts of interest.

REFERENCES

1. Palmieri V, Devereux RB, Hollywood J, Bella JN, Liu JE, Lee ET, et al. Association of pulse pressure with cardiovascular outcome is independent of left ventricular hypertrophy and systolic dysfunction: the Strong Heart study. Am J Hypertens 2006; 19:601–607.

2. Roman MJ, Devereux RB, Kizer JR, Okin PM, Lee ET, Wang W, et al. High central pulse pressure is independently associated with adverse cardiovascular outcome. The strong heart study. J Am Coll Cardiol 2009; 54:1730–1734.

3. Waddell TK, Dart AM, Medley TL, Cameron JD, Kingwell BA. Carotid pressure is a better predictor of coronary artery disease severity than brachial pressure. Hypertension 2001; 38:927–931.

4. Weber T, Auer J, O'Rourke MF, Kvas E, Lassnig E, Berent R, Eber B. Arterial stiffness, wave reflections, and the risk of coronary artery disease. Circulation 2004; 109:184–189.

5. Mitchell GF. Effects of central arterial aging on the structure and function of the peripheral vasculature: Implications for end-organ damage. J Appl Physiol (Bethesda, MD, 1985) 2008; 105:1652–1660.

6. Williams B, Lacy PS, Thom SM, Cruickshank K, Stanton A, Collier D, et al. Differential impact of blood pressure-lowering drugs on central aortic pressure and clinical outcomes: principal results of the Conduit Artery Function Evaluation (CAFE) study. Circulation 2006; 113:1213–1225.

7. Satoh H, Saijo Y, Kishi R, Tsutsui H. Brachial-ankle pulse wave velocity is an independent predictor of incident hypertension in Japanese normotensive male subjects. Environ Health Prevent Med 2011; 16:217–223.

8. Leung MC, Meredith IT, Cameron JD. Aortic stiffness affects the coronary blood flow response to percutaneous coronary intervention. Am J Physiol Heart Circ Physiol 2006; 290:H624–H630.

9. Westerhof N, Sipkema P, van den Bos GC, Elzinga G. Forward and backward waves in the arterial system. Cardiovasc Res 1972; 6:648–656.

10. Wang JJ, O'Brien AB, Shrive NG, Parker KH, Tyberg JV. Time-domain representation of ventricular-arterial coupling as a windkessel and wave system. Am J Physiol Heart Circ Physiol 2003; 284:H1358–H1368.

11. Davies JE, Alastruey J, Francis DP, Hadjiloizou N, Whinnett ZI, Manisty CH, et al. Attenuation of wave reflection by wave entrapment creates a 'horizon effect' in the human aorta. Hypertension 2012; 60:778–785.

12. Tyberg JV, Bouwmeester JC, Parker KH, Shrive NG, Wang JJ. The case for the reservoir-wave approach. Int J Cardiol 2014; 172:299–306.

13. Tyberg JV, Davies JE, Wang Z, Whitelaw WA, Flewitt JA, Shrive NG, et al. Wave intensity analysis and the development of the reservoir-wave approach. Med Biol Eng Comput 2009; 47:221–232.

14. Hughes A, Wang JJ, Bouwmeester C, Davies J, Shrive N, Tyberg J, Parker K. The reservoir-wave paradigm. J Hypertens 2012; 30:1880–1881.

15. Hope SA, Tay DB, Meredith IT, Cameron JD. Waveform dispersion, not reflection, may be the major determinant of aortic pressure wave morphology. Am J Physiol Heart Circ Physiol 2005; 289:H2497–H2502.

16. Baksi AJ, Treibel TA, Davies JE, Hadjiloizou N, Foale RA, Parker KH, et al. A meta-analysis of the mechanism of blood pressure change with aging. J Am Coll Cardiol 2009; 54:2087–2092.

17. Cheng K, Cameron JD, Tung M, Mottram PM, Meredith IT, Hope SA. Association of left ventricular motion and central augmentation index in healthy young men. J Hypertens 2012; 30:2395–2402.

18. Karamanoglu M, Feneley MP. Late systolic pressure augmentation: role of left ventricular outflow patterns. Am J Physiol 1999; 277:H481–H487.

19. Narayan O, Davies JE, Hughes AD, Dart AM, Parker KH, Reid C, Cameron JD. Central aortic reservoir-wave analysis improves prediction of cardiovascular events in elderly hypertensives. Hypertension 2015; 65:629–635.

20. Aguado-Sierra J, Alastruey J, Wang JJ, Hadjiloizou N, Davies J, Parker KH. Separation of the reservoir and wave pressure and velocity from measurements at an arbitrary location in arteries. Proceedings of the Institution of Mechanical Engineers. Part H. J Eng Med 2008; 222:403–416.

21. Parker KH, Alastruey J, Stan GB. Arterial reservoir-excess pressure and ventricular work. Med Biol Eng Comput 2012; 50:419–424.

22. Westerhof N, Segers P, Westerhof BE. Wave separation, wave intensity, the reservoir-wave concept, and the instantaneous wave-free ratio: presumptions and principles. Hypertension 2015; 66:93–98.

23. Laxminarayan S. The calculation of forward and backward waves in the arterial system. Med Biol Eng Comput 1979; 17:130.

24. Mynard JP, Smolich JJ. The case against the reservoir-wave approach. Int J Cardiol 2014; 176:1009–1012.

25. Segers P, Swillens A, Vermeersch S. Reservations on the reservoir. J Hypertens 2012; 30:676–678.

26. Davies JE, Lacy P, Tillin T, Collier D, Cruickshank JK, Francis DP, et al. Excess pressure integral predicts cardiovascular events independent of other risk factors in the conduit artery functional evaluation substudy of Anglo-Scandinavian cardiac outcomes trial. Hypertension 2014; 64:60–68.

27. Hametner B, Wassertheurer S, Hughes AD, Parker KH, Weber T, Eber B. Reservoir and excess pressures predict cardiovascular events in high-risk patients. Int J Cardiol 2014; 171:31–36.

28. Westerhof N, Westerhof BE. Crosstalk proposal: forward and backward pressure waves in the arterial system do represent reality. J Physiol 2013; 591:1167–1169.

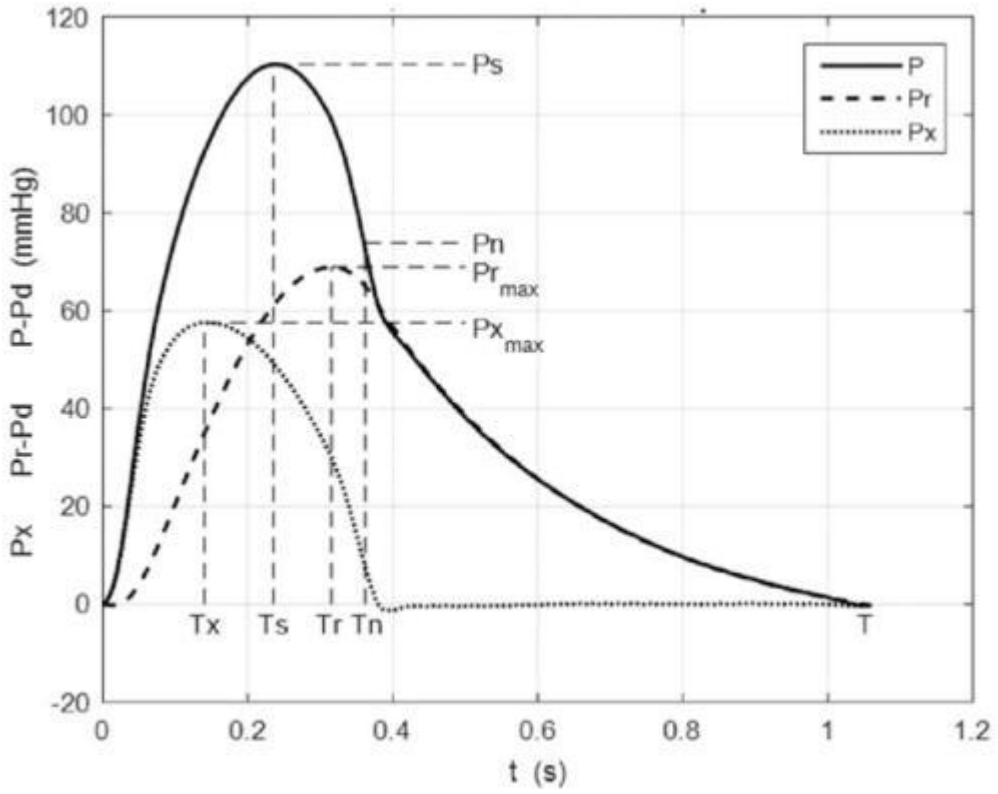

FIGURE 1. A typical example of the ensemble average pressure P (solid line), together with the reservoir pressure P_r (dashed line) and excess pressure P_x (dotted line). This example is from the aortic bifurcation (site 5). Also shown are the maxima P_s, $P_{r\,max}$ and $P_{x\,max}$, and times of the maxima, T_s, T_r and T_x, respectively. T_n is the time of minimum dP/dt after T_s, which is taken as the end of systole and P_n is the pressure at that time.

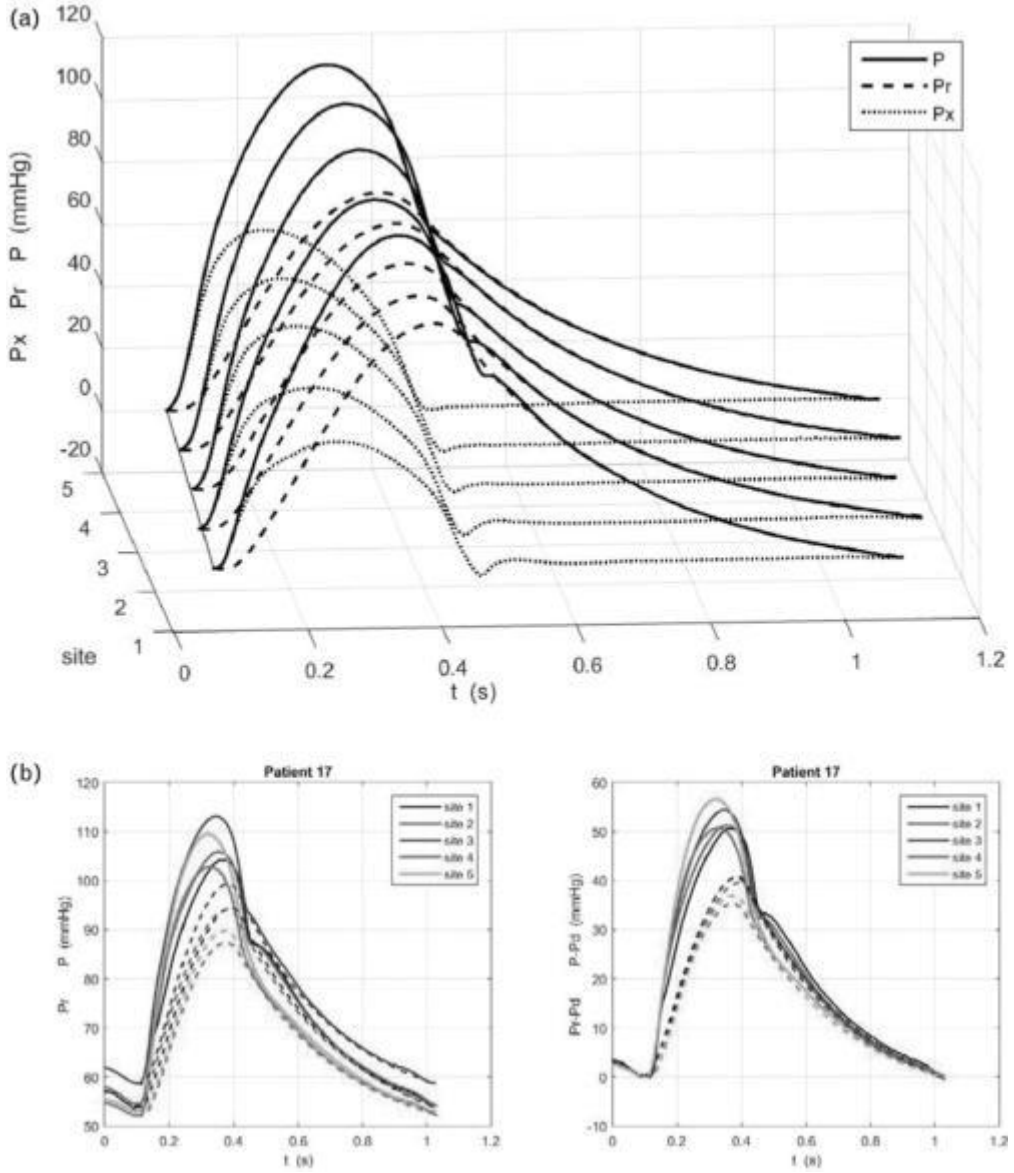

FIGURE 2. (a) The ensemble average of the measured pressure waveform at the five aortic sites for one patient (black), together with the reservoir (dashed) and excess (dotted) pressure waveforms. Time is relative to the R-wave of the simultaneously measured ECG. The dotted black line indicates the time of the diastolic point at the different sites, and the slope of this line is the pulse wave speed. For ease of comparison of the waveforms, $P–P_d$ and $P_r–P_d$ are plotted. (b) Example data from the same individual participant showing pressure waveforms at the five sites relative to atmospheric pressure (left panel); note the changes in P_d between sites. The right hand panel shows the same data plotted relative to P_d [i.e. $P(t)–P_d$ and $P_r(t)–P_d$]. The waveforms are aligned at the start of systole to allow comparison.

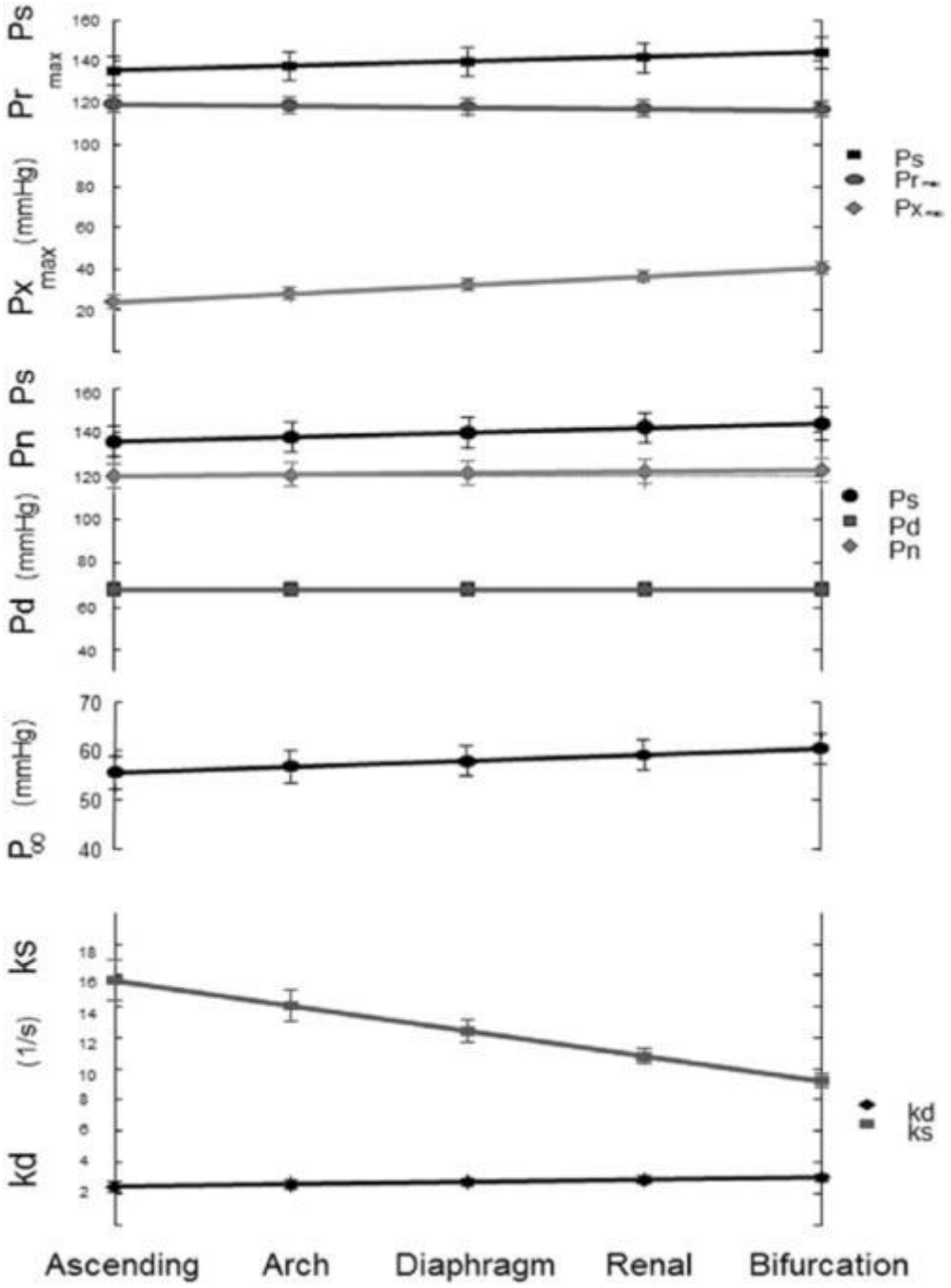

FIGURE 3. Intra-class correlation by aortic site. The symbols represent the mean values over all patients ± 95% CI. From the top: P_s – systolic pressure (mmHg); $P_{r\,max}$ – maximum reservoir pressure (mmHg); $P_{x\,max}$ – maximum excess pressure (mmHg); P_s – systolic pressure (mmHg); P_n – pressure at the end of systole (mmHg); P_d – diastolic pressure (mmHg); $P_{[infinity]}$ - asymptotic fall-off pressure (mmHg); k_s – systolic rate constant (/s), k_d – diastolic rate constant (/s).